Yilmaz *et al.*
Egyptian Journal of Forensic Sciences (2024) 14:25
https://doi.org/10.1186/s41935-024-00400-6

Egyptian Journal of Forensic Sciences

ORIGINAL ARTICLE Open Access

Sex and age estimation with corneal topography parameters by using machine learning algorithms and artificial neural networks

Nesibe Yilmaz[1*], Yusuf Secgin[1] and Kadir Mercan[2]

Abstract

Background The aim of this study, which was based on this hypothesis, was to estimate sex and age by using a machine learning algorithm (ML) and artificial neural networks (ANN) with parameters obtained from the eyeball. The study was conducted on corneal topography images of 155 women and 155 men aged between 6 and 87 who did not have surgical intervention or pathology in their eyeballs. In the study, the individuals were divided into four different age groups 6–17, 18–34, 35–55, and 56–87. Sex and age estimation was carried out by using the numerical data of parameters obtained as a result of corneal topography imaging in ML and ANN inputs.

Results As a result of our study, in sex determination, a 0.98 accuracy rate (Acc) was obtained with the logistic regression algorithm, one of the ML algorithms, and 0.94 Acc was obtained with the MLCP model, one of the ANN algorithms; in age estimation, 0.84 Acc was obtained with RF algorithm, one of the ML algorithms. With the SHAP analyzer of the Random Forest algorithm, through which the effects of parameters on the overall result are evaluated, the parameter that made the highest contribution to sex estimation was found to be corneal volume, and the parameter that made the highest contribution to age estimation was found to be pupil Q parameter.

Conclusion As a result of our study, it was found that parameters obtained from the eyeball showed a high accuracy in sex and age estimation.

Keywords Sex estimation, Age estimation, Eyeball, Machine learning algorithms, Artificial neural networks

Background

Sex and age estimation are very important for forensic, surgical, clinical medical sciences, and retail sales and marketing sectors. Knowing the age and sex of the individual is important in postmortem identification in forensic sciences and preventing child pornography; in the determination of age in forensic cases; in the determination of the risk of diseases such as glaucoma, amblyopia, cataract, hyperopia, myopia, etc. and administering the right surgical intervention in surgical and clinical sciences; and in the presentation of products to right masses in sales and marketing sectors (Bakici et al. 2021; Huynh et al. 2020; Machado et al. 2017; Rüfer et al. 2010; Secgin et al. 2022; Senol et al. 2023; Snellingen et al. 2001; Xiao et al. 2015)).

In diagnosis and treatment processes of eye diseases (keratoconus, corneal ectasia, cataract, etc.), corneal topography devices are frequently used. These devices provide detailed information about the eye by mapping

*Correspondence:
Nesibe Yilmaz
nesibeyilmaz@karabuk.edu.tr
[1] Department of Anatomy, Faculty of Medicine, Karabuk University, Karabuk, Turkey
[2] Department of Eye Diseases, Faculty of Medicine, Karabuk University, Karabuk, Turkey

the anterior corneal part of the eye extensively. It is reported that the anterior segment of the eye is measured reliably with this device (Kazancı et al. 2016; Uçakhan 2020). Interpretation of this information provided by corneal topography devices requires serious expertise. Although some of these devices have algorithm-based applications to support interpretation, their prevalence is low and there is no universally accepted software (Shanthi et al. 2022).

Using engineering-based algorithms [artificial neural networks (ANN), machine learning algorithms (ML), deep learning] as assistive in the reconstruction and interpretation of medical images, in the detection and segmentation of pathologies, in data analysis, in classifying reports and identifying morphometric data play a critical role in getting accurate results in a short time. Artificial Neural Networks is a mathematical model that can produce results for problems that consist of input, hidden, and output layers. Machine learning algorithms a modern classifiers with 2 subclasses supervised, unsupervised, and reinforced, and can detect the complex relationships between input and output. Although ML and ANN are engineering-based algorithms, they are widely used in many areas of modern medicine due to their accurate and fast decision-making (Currie et al. 2019; Oner et al. 2019; Toy et al. 2022).

The aim of this study is sex and age estimation by analyzing parameters obtained from the eyeball with modern classifiers of ANN and ML.

Methods

Study population and imaging protocol

The study was conducted with the 2023/1310 numbered decision of the Karabuk University local ethics committee. The study was conducted on 155 women and 155 men (310 individuals in total) between the ages of 6 and 87 who had healthy eyeball structures (with no surgical operation or pathology). The patients were grouped into four as 6–17 years of age (group 1), 18–34 years of age (group 2), 35–55 years of age (group 3), and 56–87 years of age (group 4) for analysis of age.

Images of the eyeball were obtained by using a CSO Sirius + (Costruzione Strumenti Oftalmici) Corneal Topography device (Scandicci, Firenze/Italy).

Image processing

Images that met the inclusion criteria and which were taken between 2022 and 2023 by CSO (Sirius +) Corneal Topography device were scanned retrospectively from Hospital Picture Archiving Communication Systems (PACS) and 15 parameters were measured by using the measurement console of the device (Fig. 1).

The parameters used in the study and their definitions are given in Table 1.

Application of machine learning algorithms and artificial neural networks

Python (Version 3.9) programming language and scikit-learn (Version 1.1.1) framework were used in ML and ANN modeling. ML and ANN models were performed by using Monster Abra A7 V12.5 model computer with 8 Gb Ram and i5 operating system. Twenty percent of the data were used as a test set and 80% were used as the training set. In ML modeling, logistic regression (LR), linear discriminant analysis (LDA), quadratic discriminant analysis (QDA), decision tree (DT), and random forest (RF) algorithms were used for sex estimation, while the RF algorithm was used for age estimation. In the ANN model, a multilayer perceptron classifier (MLCP) was used for the estimation of sex. No extraction or cleaning was applied to the raw data in order for ML and ANN models to be realistic. In MLCP, 16 neurons were used in the input layer and 2 neurons were used in the output layer for sex estimation. In addition, 2 hidden layers were preferred (48 neurons were used in the first hidden layer and 32 neurons were used in the second hidden layer). The data were retrained again 100, 200, and 1000 times so that the topologies could reflect the reality. In both models, Accuracy (Acc), Specificity (Spe), Sensitivity (Sen), and F1 score (F1) values were used for (ML-YSA) performance criteria.

$$\mathrm{Acc} = \frac{\mathrm{TP}}{\mathrm{TP} + \mathrm{FN} + \mathrm{FP} + \mathrm{TN}}$$

$$\mathrm{Sen} = \frac{\mathrm{TP}}{\mathrm{TP} + \mathrm{FN}}$$

$$\mathrm{Spe} = \frac{\mathrm{TN}}{\mathrm{TN} + \mathrm{FP}}$$

$$\mathrm{F1} = 2\frac{\mathrm{Precision} \times \mathrm{Recall}}{\mathrm{Precision} + \mathrm{Recall}}$$

Equation 1. (TP; True positive, FP; False positive, TN; True negative, FN; False negative).

LR is an extension of basic regression analysis and can model binary variables in a powerful way. DT is one of the oldest ML algorithm models that models the parameters as if they were a tree structure. In this model, there is a root node and a leaf node, and the branching continues until it reaches the lowest node. DT is easy to interpret as it shows the parameters in a tree structure. RF is an ensemble classifier and works like multiple DTs. RF differs from DT in that it evaluates different parts of the

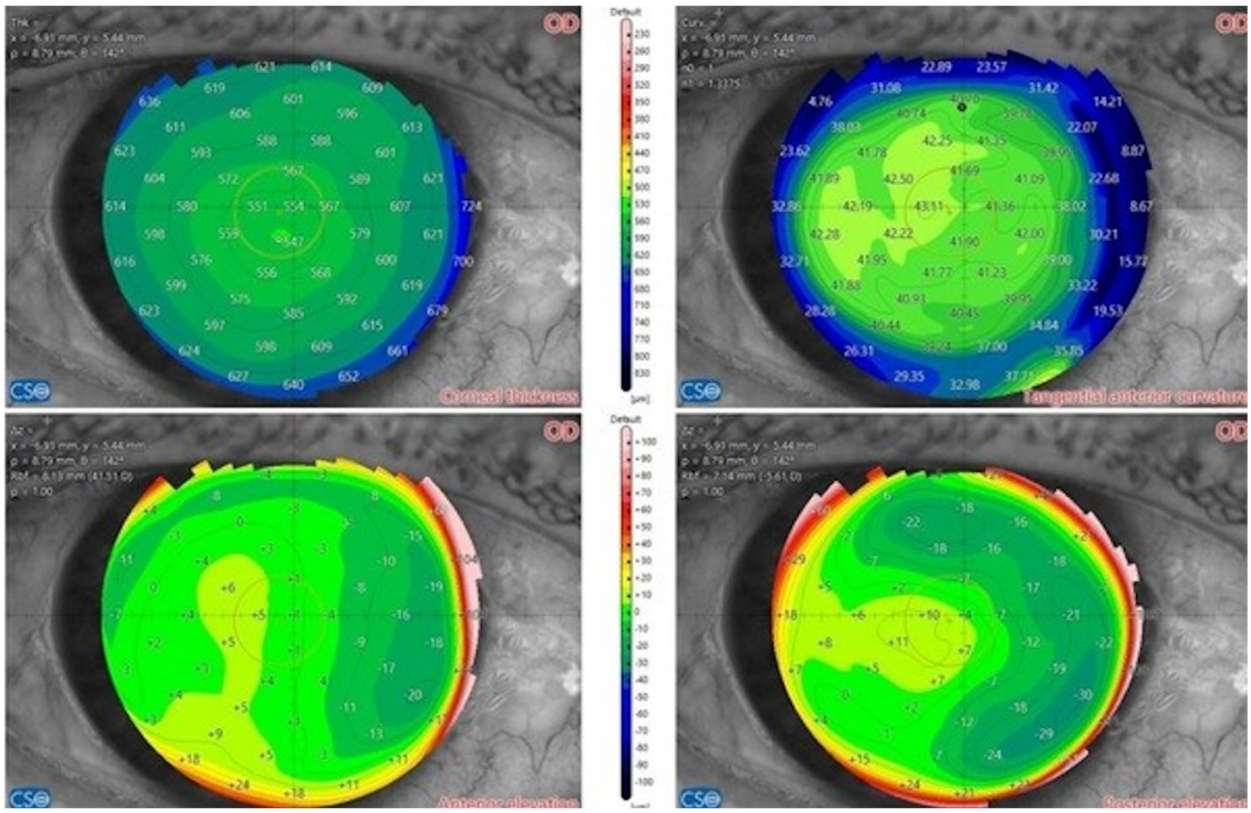

Fig. 1 CSO Sirius + corneal topography scan image showing the measured parameters

Table 1 The measured corneal topography parameters and their definitions

Parameters	Definitions
Corneal thickness (ThkMIN)	Thickness of the cornea where it is measured thinnest
Anterior corneal surface maximum keratometry value (K^{F}_{MAX})	Maximum keratometry value on the anterior corneal surface
Posterior corneal surface maximum keratometry value (K^{B}_{MAX})	Maximum keratometry value on the posterior surface of the cornea
Gullstrand ratio A/P	Refractive index ratio of the corneal surface from front to back
Gullstrand ratio P/A	Refractive index ratio of the corneal surface from back to front
Corneal volume	Volume of the cornea in a 10-mm diameter area
Pupil Q	Pupil diameter
Central corneal thickness (CCT)	Thickness of the center of the cornea in microns
Aqueous thickness (AqD)	Distance between the posterior surface of the cornea and the lens
Lens rise	Lens height
Horizontal anterior chamber depth (HACD)	The distance between the longest horizontal distance between the inner corneal surfaces and the iridocorneal angle
White to white length (W-W)	The horizontal corneal diameter, measured between the borders of the corneal limbus
Iridocorneal angle	Irodocorneal angulation
Horizontal anterior chamber tilt (HACtilt)	The two longest horizontal measurement axes
Anterior chamber volume (AC Volume)	Front chamber volume

training set and is more sensitive. LDA is a model that categorizes different classes, which is often preferred by anthropologists. QDA is a second-order parametric classifier and is superior to LDA. ANNs are so named because they resemble neurons, which are composed of axons and dendrites. The ANN is in the form of an

interconnected node (like neurons are connected to each other and neuronal transmission occurs) and these nodes are called input, output, and hidden layers according to their transformation (Curate et al. 2017; Santos et al. 2014; Toy et al. 2022; Uddin et al. 2019).

Statistical analysis

Whether the data fit normal distribution was tested with Anderson Anderson–Darling test. Median, minimum, and maximum values were included in descriptive statistics. Minitab 17 package program was used for basic statistical analyses.

Results

In the study conducted on 310 individuals between the ages of 6 and 87, it was found with the Anderson–Darling test that the parameters were not normally distributed. Table 2 shows the descriptive statistics of the parameters. ThkMIN, KFMAX, corneal volume and Pupil Q parameters median values were higher in women compared to men. KBMAX, AqD, lens rise, HACD, W-W, iridocorneal angle, HACtilt, and AC volume parameters median values were higher in men than women.

Of the ML models with which parameters were evaluated in terms of sex, the highest Acc rate was obtained as 0.98 with the LR algorithm. The accuracy of the other algorithms was between 0.76 and 0.92 (Table 3).

The confusion matrix obtained as a result of ML modeling is shown in Fig. 2a–e. In the LR algorithm with the highest accuracy rate, all 32 male individuals in the test set and 29 of the 30 female individuals were correctly predicted.

The overall effect of all parameters in terms of sex was evaluated by using the SHAP analyzer of the RF algorithm and it was found that the corneal volume parameter provided the highest contribution to accuracy (Fig. 3).

With the MLCP model, in which parameters were evaluated in terms of sex, the highest accuracy rate of 0.94 was obtained as a result of 500 trainings (Table 4). In 100- and 1000-times training, an accuracy of 0.92 was obtained.

The confusion matrix obtained as a result of ANN modeling is shown in Fig. 4. Twenty-eight of the 32 male and all of the 30 female individuals in the test set in the 500-fold learning were correctly predicted.

In age estimation with ML models, an Acc rate higher than 0.75 was obtained only with the RF algorithm, and the rate of other algorithms was ignored because they were lower than 0.75. With the RF algorithm, 0.84 Acc, 0.84 Spe, 0.84 Sen, and 0.83 F1 performance rates were obtained. The confusion matrix obtained as a result of the RF algorithm is shown in Fig. 5.

Table 2 Descriptive statistics of the measured corneal topography parameters

Parameters	Sex	Minimum	Median	Maximum
Age	Male	6.00	62.00	87.00
	Female	7.00	46.00	80.00
ThkMIN	Male	406.00	537.00	646.00
	Female	179.00	541.00	623.00
K^F_{MAX}	Male	41.20	44.75	186.49
	Female	42.39	46.09	95.56
K^B_{MAX}	Male	−10.28	−6.41	−5.83
	Female	−16.14	−6.57	−5.85
Gullstrand ratio A/P	Male	0.73	1.19	4.20
	Female	0.06	1.19	1.81
Gullstrand ratio P/A	Male	0.24	0.84	10.99
	Female	0.55	0.84	16.25
Corneal volume	Male	32.10	56.30	75.50
	Female	48.50	57.90	66.20
Pupil Q	Male	1.77	2.93	7.54
	Female	1.72	3.16	7.06
CCT	Male	0.41	0.55	0.66
	Female	0.31	0.55	0.63
AqD	Male	1.94	3.14	4.29
	Female	1.78	2.86	4.16
Lens rise	Male	-2.35	0.11	0.73
	Female	-1.15	0.03	0.63
HACD	Male	9.90	12.16	23.34
	Female	9.63	11.58	12.91
W-W	Male	9.64	12.14	44.00
	Female	10.01	11.50	14.21
Iridocorneal angle (^{0})	Male	30.90	49.00	68.30
	Female	39.20	47.30	63.50
HACtilt	Male	1.70	5.20	16.30
	Female	1.10	5.00	21.00
AC Volume	Male	105.02	178.89	280.65
	Female	88.14	164.63	259.00

* *ThkMIN* corneal thickness, K^F_{MAX} anterior corneal surface maximum keratometry value, K^B_{MAX} posterior corneal surface maximum keratometry value, *CCT* central corneal thickness, *AqD* aqueous thickness, *HACD* horizontal anterior chamber depth, *W-W* white to white length, *HACtilt* horizontal anterior chamber tilt

Table 3 Performance criteria obtained in terms of sex as a result of machine learning algorithms (for sex)

Algorithms	Acc	Spe	Sen	F1
LR	0.98	0.98	0.98	0.98
LDA	0.92	0.92	0.92	0.92
QDA	0.76	0.76	0.76	0.76
DT	0.76	0.76	0.76	0.76
RF	0.84	0.84	0.84	0.84

* *LR* logistic regression, *LDA* linear discriminant analysis, *QDA* quadratic discriminant analysis, *DT* decision tree, *RF* random forest

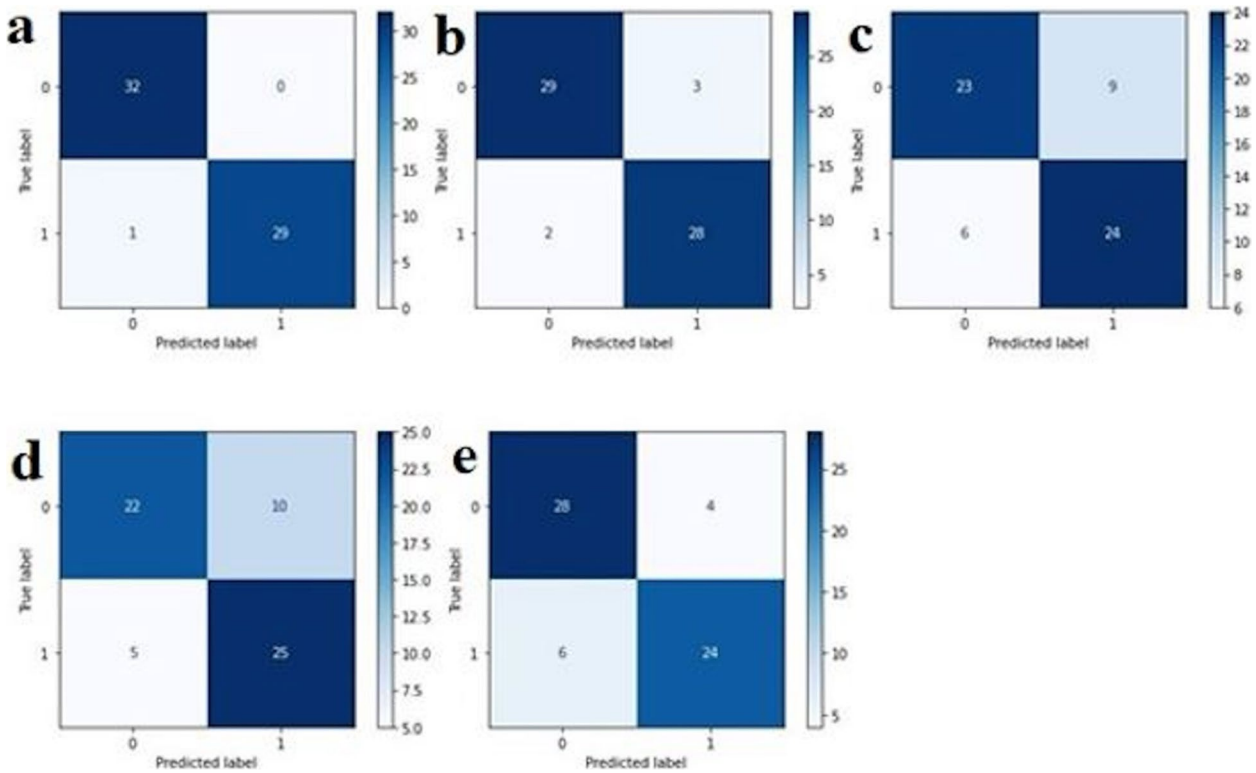

Fig. 2 Confusion matrix table of machine learning algorithms (for sex). **a** Logistic regression (LR). **b** Linear discriminant analysis (LDA). **c** Quadratic discriminant analysis (QDA). **d** Decision tree (DT). **e** Random forest (RF)). *****The number 0 represents males and 1 represents females, and 62 individuals in the confusion matrix table consist of individuals in the test set (20%)

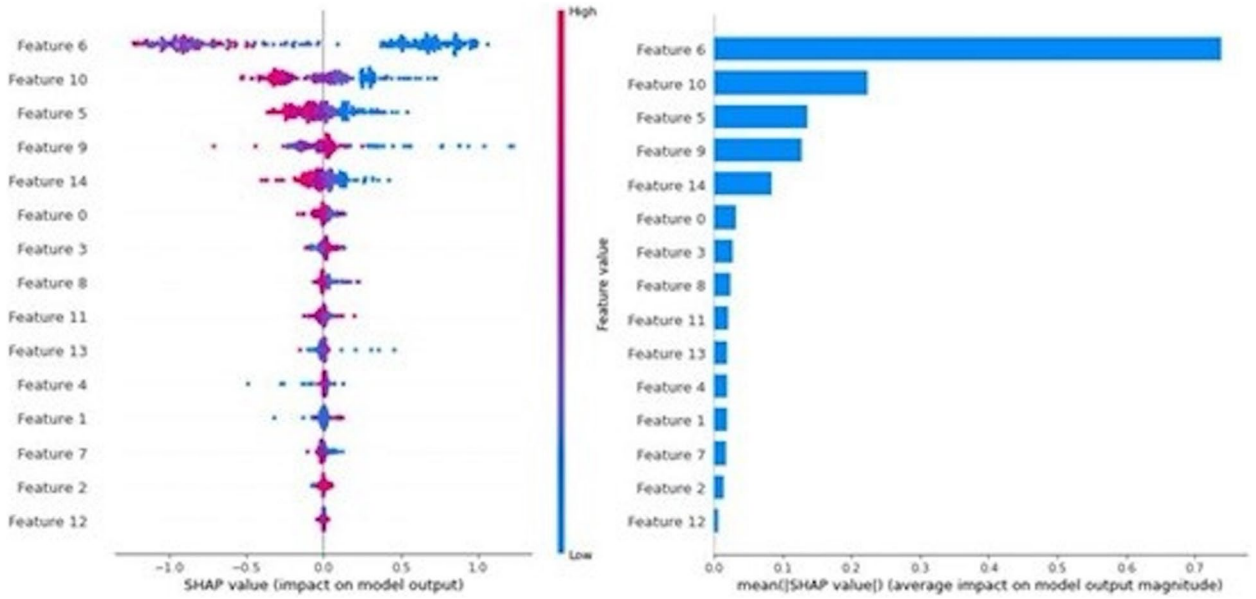

Fig. 3 SHAP analyser of the Random Forest algorithm for sex. *Feature 0: Age, 1: ThkMIN, 2: KFMAX, 3: KBMAX, 4: Gullstrand ratio A/P, 5: Gullstrand ratio, 6: Corneal volume, 7: CCT, 8: AqD, 9: Lens rise, 10: HACD, 11: W-W, 12: Iridocorneal angle, 13: HACtilt, 14: AC Volume

Table 4 Performance criteria of artificial neural network model (for sex)

Number of education	Acc	Spe	Sen	F1
100	0.92	0.92	0.92	0.92
500	0.94	0.94	0.94	0.94
1000	0.92	0.92	0.92	0.92

* *Acc* accuracy, *Spe* specificity, *Sen* sensitivity, *F1* F1 score

The overall effect of all parameters in terms of age was evaluated by using the SHAP analyzer of the RF algorithm and it was found that the Pupil Q parameter provided the highest contribution to accuracy (Fig. 6).

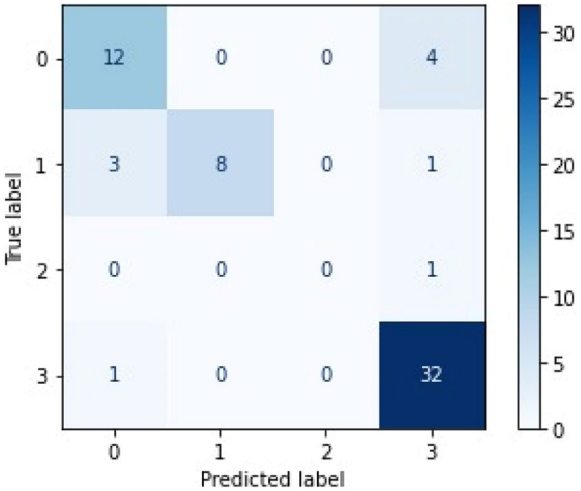

Fig. 5 Confusion matrix table of machine learning algorithm model (for age). *Number 0 represents the 1st age group (6–17 years), number 1 represents the 2nd age group (18–34 years), number 2 represents the 3rd age group (35–55 years), number 3 represents the 4th age group (56–87 years) and 62 individuals in the confusion matrix table consist of individuals in the test set (20%)

Discussion

In this study which estimated sex and age with parameters obtained from the eyeball by using ML and YSA methods, an accuracy rate between 0.76 and 0.98 was obtained in sex estimation with ML algorithms, an accuracy rate of 0.84 was obtained in age estimation with RF algorithm and an accuracy rate between 0.92 and 0.94 was obtained in sex estimation with MLCP model. With the SHAP analyzer, it was found that the parameter that made the highest contribution to sex estimation was Corneal volume, while the parameter that made the highest contribution to age estimation was pupil Q.

The eye is the center of the visual sense, about 1 inch in size, which opens the individual to the outside world. The eye receives and focuses incoming rays, converts light energy into chemical and electrical energy, and transmits this energy to the brain (Özer et al. 2016).

The structures that make up the face (eyes, mouth, nose, eyebrows) show differences depending on age and sex. These differences are among the important topics of anthropology. Among the structures that make up the face, the eye contributes greatly to the general aesthetics of the face and its sex and age-related changes (Yasaswini Paladugu 2023).

Due to normal aging of the eye, the corpus vitreum in the eye may lose its jelly-like consistency and become more liquid, the muscles may lose their tense state, and cell death may occur in the cornea and retina. As a result of these conditions, vision loss, focusing problems, decreased sharpness in the eye, narrowing of the visual field, and dry eye may occur. Environmental factors, food habits, and genetic structure affect this normal aging of the eye (Chader et al. 2013; Erdinest et al. 2021).

In eye clinics, devices that come into direct contact with the eye and devices that do not come into direct contact with the eye are used. Devices that do not come

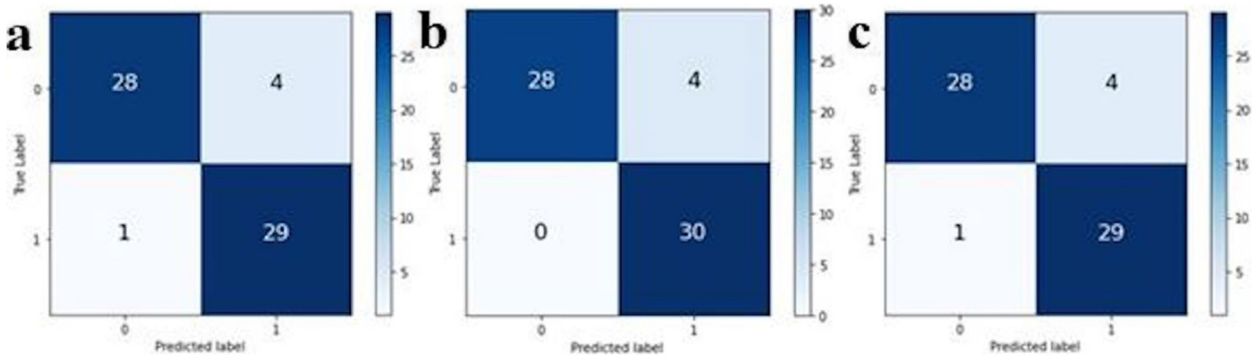

Fig. 4 Confusion matrix table of artificial neural network model (for sex). **a** 100 times training. **b** 500 times training. **c** 1000 times training)*The number 0 represents males and 1 represents females, and 62 individuals in the confusion matrix table consist of individuals in the test set (20%)

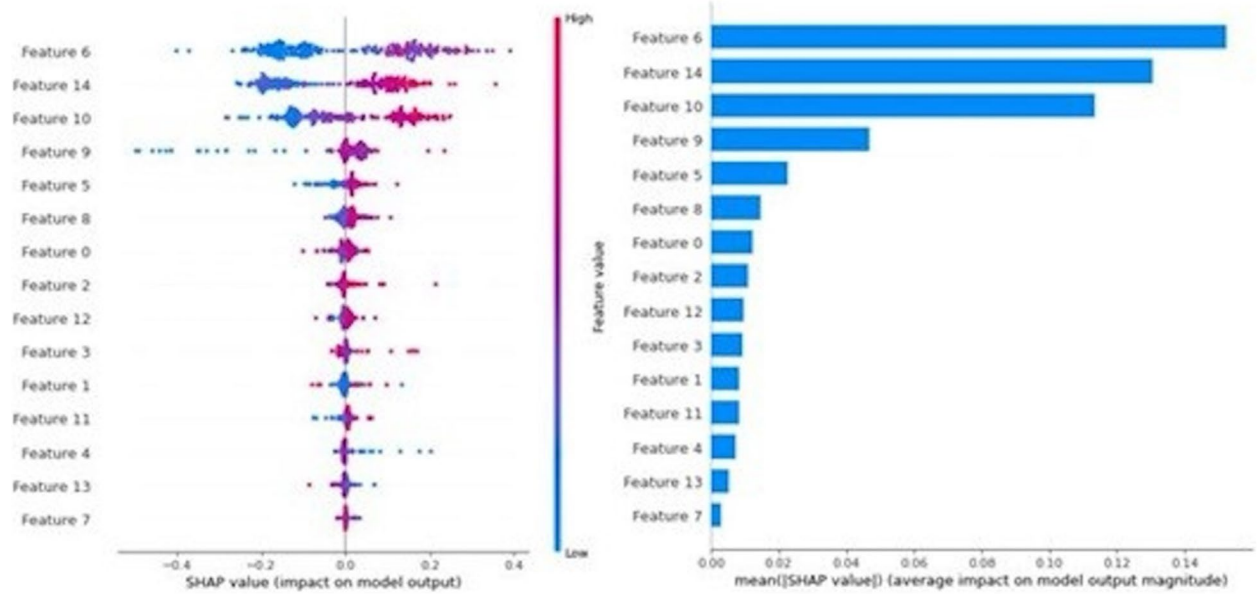

Fig. 6 SHAP analyzer of Random Forest algorithm for age * Feature 6: Pupil Q, 14: AC Volume, 10: HACD, 9: Lens rise, 5: Corneal volume, 8: AqD, 0: ThkMIN, 2: K^{B}_{MAX}, 12: Iridocorneal angle, 3: Gullstrand ratio A/P, 1: K^{F}_{MAX}, 11: W-W, 4: Gullstrand ratio P/A, 13: HACtilt, 7: CCT

into direct contact with the eye are preferred more often since there is no probability of infection and defect. A corneal topography device is a device that provides the opportunity to examine the cornea and anterior chamber in detail with 25 radial sections without direct contact with the eye. Due to this feature, this device is frequently preferred in the examination of individuals with a healthy eye structure and the diagnosis and treatment of individuals with abnormal eye structure in eye clinics (Bayramoğlu et al. 2022; Karakurt 2019; Kazancı et al. 2016; Tekin et al. 2020; Uçakhan 2020; Yıldırım et al. 2013).

In a study they conducted on 107 healthy adults by using a corneal topography device, Kazancı et al. 2016 found corneal volume as 58 ± 3.3 mm^3, CCT as 541.5 ± 31.7 µm and reported that corneal volume and CCT decreased with age. In a study they conducted on 30 healthy individuals between the ages of 10 and 53, Tekin et al. 2020 found CCT as 538.9 ± 45.2 µm. In a study they conducted on 50 individuals, Wells et al. 2013 examined CCT with optical pachymetry and found as 523.7 ± 42.3 µm. In a study they conducted on 66 glaucoma, 82 ocular hypertension patients, and 40 controls, they found the mean CCT value as 553.4 ± 37 µm and reported that there were no statistically significant differences between sexes. In a study they conducted on 28 healthy, 28 atopic dermatitis patients, Yıldırım et al. 2013 found CCT in the healthy group as 565.1 ± 22 µm. In a study they conducted on 52 healthy individuals, Gonzalez-Perez et al. 2018 found the mean CCT as 550.4 ± 30.5 µm. In our study, the median value of the corneal volume parameter was 56.30 mm^3 in men and 57.90 mm^3 in women; the median value of the CCT parameter was 0.55 in men and women. In addition, it was found that the highest contribution among the parameters we used in sex estimation was by corneal volume and this parameter was the fifth in age estimation. These studies in the literature support our results morphometrically.

In a study they conducted on 303 healthy individuals between the ages of 10 and 70, Karakurt et al. 2019 grouped individuals into 7 according to their ages; they found AC volume parameter was between 146.07 ± 48.30 mm^3 and 215.27 ± 62.68 mm^3 according to age groups, AC volume parameter was reversely correlated with age and it did not have a significant correlation with sex. In a study they conducted on 73 pediatric individuals, Bayramoğlu et al. 2022 found the AC volume value as 159 ± 25 mm^3. In our study, we found median AC volume as 178.89 mm^3 in men and as 164.63 mm^3 in women and we found that it had the 10th effect among all parameters we used to determine sex and the 2nd effect in determination of age. This shows that the AC volume parameter is an important variable in terms of age.

In a study they conducted on 112 healthy individuals between the ages of 15 and 65, Kalaycı et al. 2014 found iridocorneal angle as 41.55 ± 6.39°, CCT as 532.11 ± 36.76 µm, AC volume as 160.43 ± 43.09 mm^3. In our study, we found the median iridocorneal angle value as 49.00° in men and 47.30° in women, the median CCT value as 0.55 in men and women, the median AC volume

as 178.89 mm^3 in men and 164.63 mm^3 in women. The literature supports our study morphometrically. In our study, the iridocorneal angle parameter contributed 10th in determining sex and 9th in determining age.

Conclusions

In this study, where sex and age were estimated with parameters obtained from the eyeball, very high accuracy rates were obtained with ANN and ML models. In this respect, we believe that the results will make great contributions to forensic, basic medical sciences, and sales sectors (eyewear, medicine, aesthetics, etc. based on the eyeball).

Abbreviations

ML	Machine learning algorithm
ANN	Artificial neural networks
MLCP	Multilayer perceptron classifier
LR	Logistic regression
DT	Decision Tree
RF	Random Forest
LDA	Linear discriminant analysis
QDA	Quadratic discriminant analysis
Acc	Accuracy
Spe	Specificity
Sen	Sensitivity
F1	F1 score
FP	False positive
FN	False negative
TP	True positive
TN	True negative
ThkMIN	Corneal thickness
K^F_{MAX}	Anterior corneal surface maximum keratometry value
K^B_{MAX}	Posterior corneal surface maximum keratometry value
CCT	Central corneal thickness
AqD	Aqueous thickness
HACD	Horizontal anterior chamber depth
W-W	White to white length
HACtilt	Horizontal anterior chamber tilt
AC Volume	Anterior chamber volume

Acknowledgements
Thanks to all the authors.

Authors' contributions
All authors contributed to the article's writing. Image acquisition: K.M; data analysis: Y.S; designed by N.Y, Y.S, and K.M. All authors read and approved the final manuscript.

Funding
No financial support has been received from any institution or organization.

Availability of data and materials
The datasets generated and/or analyzed during the current study are not publicly available due (reason why data are not public) but are available from the corresponding author on reasonable request.

Declarations

Ethics approval and consent to participate
Approval was obtained from the Karabuk University Non-Interventional Ethics Committee with decision no. 2023–1310. informed consent include appropriate statements.

Consent for publication
Not applicable.

Competing interests
The authors declare that they have no competing interests.

Received: 12 July 2023 Accepted: 31 May 2024
Published online: 11 June 2024

References

Bakici RS, Oner Z, Oner S (2021) The analysis of sacrum and coccyx length measured with computerized tomography images depending on sex. Egypt J Forensic Sci 11(1):1–13
Bayramoğlu SE, Erdoğan M, Sarici K, Artış G, Özdemir A, Sayın N (2022) Pediyatrik Popülasyonda, Endotelyal Hücre Yoğunluğunun ve Morfolojisinin, Topografik Ön Segment Parametreleri ile İlişkisi. İstanbul Kanuni Sultan Süleyman Tıp Dergisi 14(1):70–76
Chader GJ, Taylor A (2013) Preface: the aging eye: normal changes, age-related diseases, and sight-saving approaches. Investigative ophthalmology & visual science 54(14):ORSF1–ORSF4
Curate F, Umbelino C, Perinha A, Nogueira C, Silva AM, Cunha E (2017) Sex determination from the femur in Portuguese populations with classical and machine-learning classifiers. J Forensic Leg Med 52:75–81
Currie G, Hawk KE, Rohren E, Vial A, Klein R (2019) Machine learning and deep learning in medical imaging: intelligent imaging. Journal of Medical Imaging and Radiation Sciences 50(4):477–487
Erdinest N, London N, Lavy I, Morad Y, Levinger N (2021) Vision through Healthy Aging Eyes. Vision 5(4):46
González-Pérez J, Queiruga Piñeiro J, Sánchez García Á, González Méijome JM (2018) Comparison of central corneal thickness measured by standard ultrasound pachymetry, corneal topography, tono-pachymetry and anterior segment optical coherence tomography. Curr Eye Res 43(7):866–872
Huynh HT, Nguyen H (2020) Joint age estimation and gender classification of Asian faces using wide ResNet. SN Computer Science 1(5):284
Kalaycı M, Güneş A, Özertürk Y (2014) Sağlıklı Gözlerde Scheimpflug Kamera ve Placido Disk Topografi ile Santral Kornea Kalınlığı Ön Kamara Derinliği Ön Kamara Hacmi ve İridokorneal Açı Değerlendirilmesi. MN Oftalmoloji 21(1):1–3
Karakurt Y (2019) Erzincan İli ve Çevresinde Yaşayan Sağlıklı Bireylerde Speküler Mikroskop ve Korneal Topografi Cihazları ile Elde Edilen Ön Segment Parametreleri Üzerine Yaş ve Cinsiyet Etkisinin Değerlendirilmesi. Gümüşhane Üniversitesi Sağlık Bilimleri Dergisi 8(1):1–9
Kazancı L, Eren S, Aydın E, Yüksel B (2016) Evaluation of Cornea and Anterior Chamber Measurements Using Sirius® Topographer in Adults. Journal of Glaucoma-Cataract 11(4):225–229
Machado CEP, Flores MRP, Lima LNC, Tinoco RLR, Franco A, Bezerra ACB, Guimarães MA (2017) A new approach for the analysis of facial growth and age estimation: Iris ratio. Plos one 12(7):e0180330
Oner Z, Turan MK, Oner S, Secgin Y, Sahin B (2019) Sex estimation using sternum part lenghts by means of artificial neural networks. Forensic Sci Int 301:6–11
Özer CM, Öz II, Serifoglu I, Büyükuysal MÇ, Barut Ç (2016) Evaluation of eyeball and orbit in relation to gender and age. Journal of Craniofacial Surgery 27(8):e793–e800
Rüfer F, Schröder A, Klettner A, Frimpong-Boateng A, Roider JB, Erb C (2010) Anterior chamber depth and iridocorneal angle in healthy White subjects: effects of age, gender and refraction. Acta Ophthalmol 88(8):885–890
Santos F, Guyomarc'h P, Bruzek J (2014) Statistical sex determination from craniometrics: Comparison of linear discriminant analysis, logistic regression, and support vector machines. Forensic science international 245(204):e201-204 (e208)
Secgin Y, Oner Z, Turan MK, Oner S (2022) Gender prediction with the parameters obtained from pelvis computed tomography images and machine learning algorithms. Journal of the Anatomical Society of India 71(3):204–209
Senol D, Secgin Y, Duman BS, Toy S, Oner Z (2023) Sex and age estimation with machine learning algorithms with parameters obtained from cone beam computed tomography images of maxillary first molar and canine teeth. Egypt J Forensic Sci 13(1):1–9

Shanthi S, Aruljyothi L, Balasundaram MB, Janakiraman A, Nirmaladevi K, Pyingkodi M (2022) Artificial intelligence applications in different imaging modalities for corneal topography. Surv Ophthalmol 67(3):801–816
Snellingen T, Rao GN, Shrestha JK, Huq F, Cheng H (2001) Quantitative and morphological characteristics of the human corneal endothelium in relation to age, gender, and ethnicity in cataract populations of South Asia. Cornea 20(1):55–58
Tekin S, Seven E, Gülbay S, Batur M, Özer M (2020) Comparison of Central Corneal Thickness Measurements by Optical Coherence Tomography, Corneal Topography and Non-Contact Specular Microscope. Van Med J 27(3):331–334
Toy S, Secgin Y, Oner Z, Turan MK, Oner S, Senol D (2022) A study on sex estimation by using machine learning algorithms with parameters obtained from computerized tomography images of the cranium. Sci Rep 12(1):4278
Ucakhan Ö (2020) Current corneal topography/tomography systems. Eye & Contact Lens 46(3):127–128
Uddin S, Khan A, Hossain ME, Moni MA (2019) Comparing different supervised machine learning algorithms for disease prediction. BMC Med Inform Decis Mak 19(1):1–16
Wells M, Wu N, Kokkinakis J, Sutton G (2013) Correlation of central corneal thickness measurements using Topcon TRK-1P, Zeiss Visante AS-OCT and DGH Pachmate 55 handheld ultrasonic pachymeter. Clin Exp Optom 96(4):385–387
Xiao, O., Morgan, I. G., Ellwein, L. B., He, M., & Group, R. E. S. i. C. S (2015) Prevalence of amblyopia in school-aged children and variations by age, gender, and ethnicity in a multi-country refractive error study. Ophthalmology 122(9):1924–1931
Yasaswini Paladugu DRS (2023) End-To-End Gender Determination By Images Of An Human Eye. Journal of Survey in Fisheries Sciences 10(2S):394–405
Yıldırım Y, Kara N, Yılmaz T, Demircan A, Çankaya İ, Kutlubay Z, Serdaroğlu S (2013) Comparison of corneal topographical and biomechanical properties in cases with atopic dermatitis and healthy subjects. Turk J Ophthalmol 43(3):140–144

Publisher's Note